I&EC research
Industrial & Engineering Chemistry Research

Article

Cite This: Ind. Eng. Chem. Res. 2019, 58, 11498−11505

pubs.acs.org/IECR

Multiclass Diagnosis of Neurodegenerative Diseases: A Neuroimaging Machine-Learning-Based Approach†

Gurpreet Singh,[‡] Meet Vadera,[§,∥] Lakshminarayanan Samavedham,[*,⊥] and Erle Chuen-Hian Lim[#]

[‡]Dalio Institute of Cardiovascular Imaging, Weill Cornell Medicine, New York, New York 10021, United States
[§]Department of Mechanical Engineering, Indian Institute of Technology Gandhinagar, Gandhinagar, Gujarat 382355, India
[∥]Department of Computer Science, University of Massachusetts, Amherst, Massachusetts 01002, United States
[⊥]Department of Chemical and Biomolecular Engineering, National University of Singapore, 117585 Singapore
[#]Division of Neurology, National University Health System, 119228 Singapore

Supporting Information

ABSTRACT: With the advent of powerful analysis tools, intelligent medical diagnostics for neurodegenerative disease (NDs) diagnosis are coming close to becoming a reality. In this work, we describe a state-of-the-art machine-learning system with multiclass diagnostic capabilities for the diagnosis of NDs. Our framework for multiclass subject classification comprises feature extraction using principal component analysis, feature selection using Fisher discriminant ratio, and subject classification using least-squares support vector machines. A multisite, multiscanner data set containing 2540 patients clinically diagnosed as Alzheimer Disease (AD), healthy controls (HC), Parkinson disease (PD), mild cognitive impairment (MCI), and scans without evidence of dopaminergic deficit (SWEDD) was obtained from Parkinson's Progression Marker Initiative and Alzheimer's Disease Neuroimaging Initiative. Our work assumes significance since studies have primarily focused on comparing only two subject classes at once, i.e., as binary classes. To profile the diagnostic capabilities for real-time clinical practice, we tested our framework for multiclass disease diagnostic capabilities. The proposed method has been trained and tested on this cohort (2540 subjects), the largest reported so far in the literature. For multiclass diagnosis, our method results in highest reported classification accuracy of 87.89 ± 03.98% with a precision of 82.54 ± 08.85%. Also, we have obtained accuracy of up to 100% for binary class classification of NDs. We believe that this study takes us one step closer to translating machine learning into routine clinical settings as a decision support system for ND diagnosis.

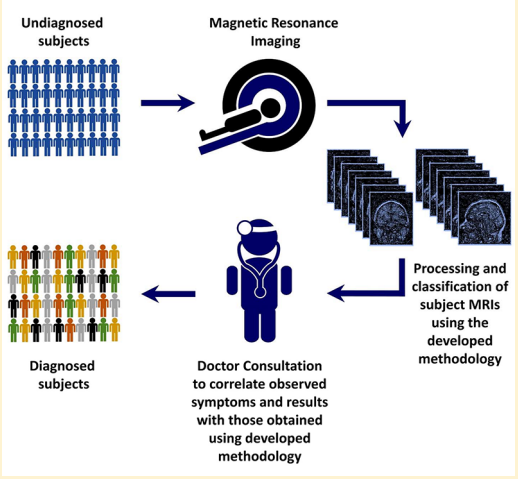

1. INTRODUCTION

The World Alzheimer Report (2015) estimated that globally there were 46.8 million people living with some form of dementia. Alzheimer's disease (AD) and Parkinson's disease (PD) are the two most prevalent progressive neurodegenerative diseases (NDs).[1] Diagnosing these diseases is challenging due to (i) similarity in the pathological symptoms between different forms of dementia especially at early stages, (ii) lack of disease-specific early detection biomarkers, (iii) complete reliance on the expertise of clinicians, and (iv) nonavailability of clinical decision support system to assist in clinical decisions for NDs. ND diagnosis, especially in the early stages, remains a formidable challenge and misdiagnosed patients lead poor disease management outcomes. Clearly, there is an urgent need to develop tests(s) and/or technique(s) that can assist in clinical decisions to enable early and accurate diagnosis.

Several studies have reported potential biomarkers for differential diagnosis of Alzheimer and Parkinson disease from other similar disorders[2,3] using group-level analysis. These findings are interesting from a research perspective but find limited use for individual-level routine clinical diagnosis. To achieve individual-level disease diagnosis, development of machine-learning-based classification algorithms is increasingly becoming an active area of neuroscience research. Machine-learning algorithms can typically handle high-dimensional multivariate data sets such as those generated from magnetic resonance imaging (MRI) scans. From these images, extraction of key features to enhance the separability between the disease classes under consideration is the key challenge for developing reliable models for ND diagnosis. These features are then fed into classification algorithms such as support vector machine[4]

Special Issue: Sirish Shah Festschrift

Received: December 15, 2018
Revised: March 29, 2019
Accepted: May 11, 2019
Published: May 12, 2019

DOI: 10.1021/acs.iecr.8b06064
Ind. Eng. Chem. Res. 2019, 58, 11498−11505

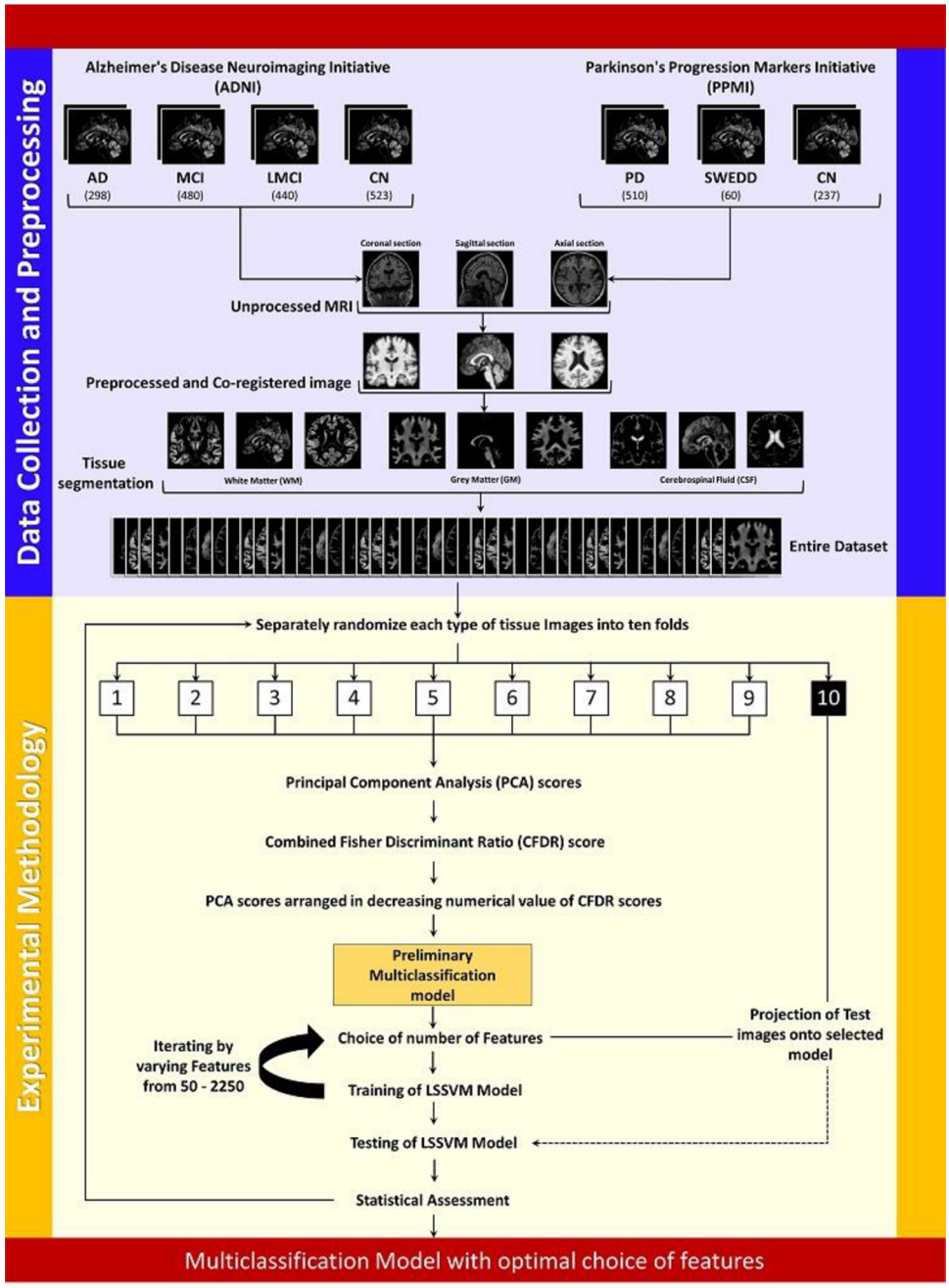

Figure 1. Graphical summary of methodology developed in this study.

and least-squares support vector machine (LSSVM)[5] for subject classification.

Classically, predetermined medical diagnosis information is used to sets of binary classes such as one for categorizing AD from healthy control (HC) or AD from mild cognitive impairment (MCI) or PD from scans without evidence of dopaminergic deficit (SWEDD) subjects. In a real scenario, establishing the disease diagnosis in a clinic is a multiclass classification problem. However, it is difficult to extend workflows designed for a simplified binary classification problem to multiple classes.[6] Thus, to move forward in the direction of realizing a real-time clinical decision support system, we propose here a novel framework to handle multiclass classification problems for diagnosing AD and PD from other similar diseases. In essence, for feature extraction, we have used principal component analysis, and then the interclass discriminative ability of the selected features was quantified using the Fisher discriminant ratio. Features were then arranged in descending order by their combined Fisher discriminant ratio scores and fed into a multiclass LSSVM for classification. To the best of our knowledge, this is the largest cohort of patients reported in the literature so far. The proposed methodology has been thoroughly tested on a data set of 2540 patients for AD, MCI, PD, SWEDD, and HC patients obtained from multiple sites and scanners. This was aimed at evaluating the generalizability of the proposed methodology for application across different sites and adaptability to scanners from different vendors.

DOI: 10.1021/acs.iecr.8b06064
Ind. Eng. Chem. Res. 2019, 58, 11498−11505

Table 1. Clinical and Demographic Details of Subjects

	subject class					
variables	AD	HC	LMCI	MCI	PD	SWEDD
M/F	144/146	410/350	357/83	284/196	339/171	38/22
age	75.92 ± 07.88	72.51 ± 11.32	75.97 ± 07.39	75.76 ± 08.02	61.78 ± 09.64	60.83 ± 10.97
education	14.27 ± 02.97	16.01 ± 02.90	15.95 ± 02.95	15.86 ± 02.57	16.00 ± 00.00	14.82 ± 03.73
MoCA		27.63 ± 01.52			26.58 ± 02.40	26.37 ± 02.40
GDS	06.32 ± 01.21	05.36 ± 01.43	05.09 ± 02.37	06.15 ± 01.60	05.42 ± 01.18	05.50 ± 01.48
Bjlo		25.72 ± 03.49			25.07 ± 03.84	25.21 ± 04.14
MDS-UPDRS		03.94 ± 03.54			26.62 ± 07.35	21.37 ± 10.58
H&Y		00.04 ± 00.20			01.73 ± 00.43	01.32 ± 00.63
MMSE	22.00 ± 02.90	28.50 ± 01.00	25.76 ± 02.99	25.31 ± 02.98		
MHIS	00.70 ± 00.69	00.58 ± 00.71	00.59 ± 00.71	00.65 ± 00.77		

[a]Data are presented as mean ± standard deviation. M/F: male/female; GDS: geriatric depression scale; MMSE: mini mental state examination; MoCA: Montreal cognitive assessment; Bjol: Benton judgment of line orientation; MDS-UPDRS: Movement Disorder Society-unified Parkinson's disease rating scale; H&Y: Hoehn and Yahr scale; MHIS: modified Hachinski Ischemia score.

2. MATERIALS AND METHODS

Steps described in this section were performed in accordance with previously validated and published studies.[5,7,8] Multicenter, multiscanner MRIs from two clinical repositories, Alzheimer's Disease Neuroimaging Initiative (ADNI) and Parkinson's Progression Marker Initiative (PPMI), were obtained for disease classes, viz., AD, MCI, PD, SWEDD, and HC subjects. These images were preprocessed to remove artifacts and coregistered to a common ICBM template. Thereafter, all the images were segmented into gray matter (GM), white matter (WM), and cerebrospinal fluid (CSF) images. These tissue-wise images of disease classes were then used to calculate PCA scores for training set of data. Combined Fischer discriminant ratio scores were then calculated to obtain statistical significance of the PCA features to improve class discriminating ability of the model. PCA scores were then arranged as per the decreasing order of combined FDR scores. This formed the preliminary multiclassification model. Decisions on optimal number of features were made by varying the number of features from 50 to 2250 and then presenting them to the LSSVM model; a 10-fold cross-validation and statistical assessment of the results was then made by calculating the accuracy, precision, sensitivity, specificity, and Mathews correlation coefficient (MCC). The model with highest accuracy and MCC was selected for binary classification whereas accuracy and precision were used for selecting model for multiclass classification. Detailed information regarding the subjects is provided in the Supporting Information. Please refer to Figure 1 for a graphical summary of methodology developed in this study.

2.1. Data Acquisition. A total of 2540 T1-weighted MRIs for AD, HC, MCI, PD, and SWEDD subjects were obtained from the Alzheimer's disease neuroimaging initiative and the Parkinson progression marker initiative. The unique features of the data set used in this study are as follows: (1) acquisition of MRIs from multiple sites and scanners and (2) MRIs obtained at both 1.5 and 3T. Table 1 presents demographic and clinical details of the subjects. Several motor and nonmotor characteristics were assessed using various tests.

2.2. Image Preprocessing. To account for the differences in the size of the brain among individuals,[9] brain MRIs were coregistered with the brain template from the International Consortium for Brain Mapping.[10] Thereafter, every MRI was smoothed and segmented to produce white matter (WM), gray matter (GM), and cerebrospinal fluid (CSF) brain images using Voxel-Based Morphometry toolbox v8.0[11] for Statistical Parametric Mapping v8.0.[12]

2.3. Feature Extraction. The resolution of MRIs obtained after preprocessing was 121 × 145 × 121 voxels. We were mindful of the fact that there exists similarity in some of the brain areas between all subjects, even between diseased and healthy control subjects. Thus, while some of the features, i.e., brain areas, might be more important to distinguish between the subjects, others might be redundant. Removal of these redundant features has 2-fold benefits. First, it speeds up the process of learning by reducing the computational load. Second, the removal of redundant features is believed to improve the accuracy of classification.[13]

We have used principal component analysis for dimensionality reduction. In this, an orthogonal transformation is applied to choose a new coordinate system such that the principal components are arranged by decreasing order of the variance in the data captured by them. Thus, the later components can be eliminated leading to a reduction in data dimensionality with minimal loss of information. For calculation of principal components, starting from the calculation of covariance matrix as shown in eq 1, we determine its eigenvalues and eigenvectors. The greater the eigenvalue of an eigenvector, the higher the variance captured from the data set by that principal component.

$$C = X \times X^T \tag{1}$$

where X is the mean centered and variance normalized data matrix and C is the calculated covariance matrix.

2.4. Feature Selection. To enhance the sensitivity of separation between the subject classes, especially for multiclass classification, we have modified the use of Fisher discriminant ratio to suit our needs for multiclass classification (see eq 2). To determine the features with higher discriminative ability, Fisher discriminant ratio scores for all the combination of classes were summed to obtain a combined score. Thereafter, the combined score values were arranged in the descending order such that the feature with the highest value has the highest discriminative ability to differentiate between subject classes under consideration.

$$\mathrm{CFDR} = \sum_{i}^{M} \sum_{j \neq i}^{M} \frac{(\mu_i - \mu_j)^2}{(\sigma_i^2 + \sigma_j^2)} \tag{2}$$

where M refers to the number of classes, (μ_i, μ_j) are the means, and (σ_i^2, σ_j^2) are the variances of the class under consideration. In

DOI: 10.1021/acs.iecr.8b06064
Ind. Eng. Chem. Res. 2019, 58, 11498−11505

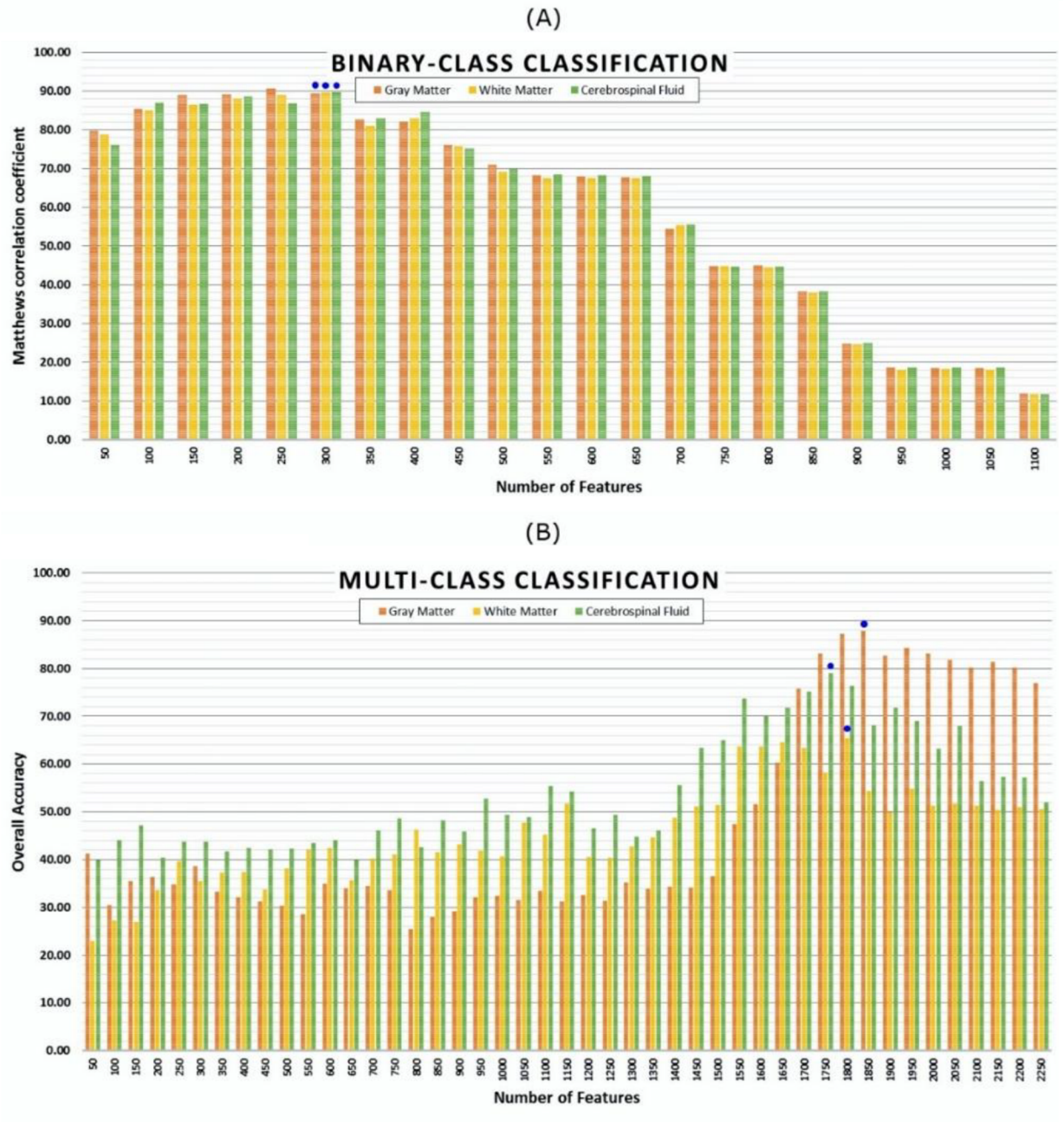

Figure 2. Average classification accuracy obtained upon varying number of principal components presented to LS-SVM for classification. "●" indicates the chosen number of features for binary and multiclass comparisons.

this work, $M = 2$ for binary classification and $M = 6$ for multiclass classification.

2.5. Feature Classification. Least-square support vector machine (LSSVM) is a reformulation of support vector machine that performs computationally faster as compared to the latter. It calculates the separation boundary between classes by calculating a solution to a set of linear equations, unlike solution to a quadratic problem. Thus, a multiclass classification problem is computationally less intensive when classifying large data sets. Mathematical formulation and details regarding LSSVM can be found elsewhere.[14]

We have used RBF kernel function and used a multidimensional unconstrained nonlinear optimization to tune the LSSVM parameters.

3. RESULTS AND DISCUSSION

3.1. Choice of Optimal Features. Classification performance is critically reliant on the number of features presented to the classifier. To find the optimal choice of features that would provide the best overall performance, the number of features were varied from 50 to the maximum number of features available in the model obtained from the principal component analysis. At each run, features were presented to LSSVM, and the performance of the classifier was evaluated (see Figure 2). For binary classification, we found 300 principal components to be optimal for all the disease classes and types of brain tissue. For multiclass classification, we found 1850, 1800, and 1750 principal components to be optimal for GM, WM, and CSF images, respectively.

DOI: 10.1021/acs.iecr.8b06064
Ind. Eng. Chem. Res. 2019, 58, 11498−11505

Table 2. Accuracy Rates Obtained for Binary and Multiclass Comparison between Subjects

comparison	accuracy	MCC	sensitivity	specificity	brain matter
AD vs HC	99.81 ± 00.43	1.00 ± 0.01	99.31 ± 01.54	100.00 ± 00.00	GM
AD vs LMCI	99.73 ± 00.61	0.99 ± 0.01	99.31 ± 01.54	100.00 ± 00.00	CSF
AD vs MCI	98.70 ± 00.92	0.97 ± 0.02	96.21 ± 03.12	100.00 ± 00.00	GM
LMCI vs HC	99.50 ± 00.46	0.99 ± 0.01	99.48 ± 00.71	99.46 ± 01.21	GM
LMCI vs MCI	99.35 ± 00.60	0.99 ± 0.01	99.50 ± 01.12	99.16 ± 01.15	WM
MCI vs HC	100.00 ± 00.00	1.00 ± 0.00	100.00 ± 00.00	100.00 ± 00.00	GM
PD vs HC	90.87 ± 02.46	0.82 ± 0.04	96.99 ± 01.13	84.11 ± 04.58	GM
PD vs SWEDD	85.61 ± 05.02	0.42 ± 0.14	95.76 ± 01.52	39.16 ± 15.96	CSF
SWEDD vs HC	92.20 ± 03.72	0.63 ± 0.13	99.43 ± 00.78	47.85 ± 14.81	WM
comparison		accuracy	precision		brain matter
AD vs LMCI vs MCI vs PD vs SWEDD vs HC		87.89 ± 03.98	82.54 ± 08.85		GM
		65.39 ± 17.47	62.89 ± 14.85		WM
		78.97 ± 12.87	75.31 ± 11.54		CSF

[a]Data are presented as mean ± standard deviation. Here we present the best results obtained for each binary comparison. Please refer to Table S1 for brain matter wise accuracy results for all the comparisons.

Table 3. Studies Investigating Binary and Multiclass Comparison for Diagnosing NDs[a]

comparison	*N*	accuracy	sensitivity	specificity	ref
AD vs HC	75/75	92			17
	23/23	94	96	92	18
	20/25	100	100	100	21
	290/760	**99.81 ± 00.43**	**99.31 ± 01.54**	**100.00 ± 00.00**	**this study**
AD vs MCI	53/52	95			19
	21/15	87	85	80	15
	290/480	**98.70 ± 00.92**	**96.21 ± 03.12**	**100.00 ± 00.00**	**this study**
MCI vs HC	15/20	95	93	90	15
	79/204	71.09	51.96	78.4	16
	23/25	83	83	84	18
	24/18	97.62	96	100	27
	480/760	**100.00 ± 00.00**	**100.00 ± 00.00**	**100.00 ± 00.00**	**this study**
PD vs HC	114/53	88			19
	510/760	**90.87 ± 02.46**	**96.99 ± 01.13**	**84.11 ± 04.58**	**this study**
	28/28	85.8	86	86	4
PD vs SWEDD	518/245	93.25 ± 0.46	97.12	85.03	5
	510/60	**85.61 ± 05.02**	**95.76 ± 01.52**	**39.16 ± 15.96**	**this study**
	518/68	99.86 ± 0.10	100	98.81	5
SWEDD vs HC	**50/760**	**92.20 ± 03.72**	**99.43 ± 00.78**	**47.85 ± 14.81**	**this study**
	68/245	100.00 ± 0.00	100	100	5
comparison	*N*	accuracy	precision		ref
AD vs MCI vs HC	180/374/204	46.30 ± 4.24			22
AD vs MCI vs HC	51/99/52	68.31 ± 1.23			20
AD vs FTD vs VaD vs DLB vs HC	223/92/24/47/118	51.6			24
AD vs FTD vs VaD vs DLB vs SMC	219/92/24/47/118	75.2			25
AD vs FTD vs VaD vs DLB vs SMC	219/92/24/47/118	82.3			26
AD vs LMCI vs MCI vs PD vs SWEDD vs HC	**290/440/480/510/60/760**	**87.89 ± 03.98**	**82.54 ± 08.85**		**this study**

[a]Data are presented as mean ± standard deviation. *N*: number; AD: Alzheimer Disease; DLB: dementia with Lewy bodies; FTLD: frontotemporal lobe degeneration; HC: healthy control subjects; LMCI: late mild cognitive impairment; MCI: mild cognitive impairment; PD: Parkinson disease; SMC: subjective memory complaints; SWEDD: scans without evidence of dopaminergic deficit; VaD: vascular dementia.

3.2. Performance Evaluation. As mentioned earlier, we performed 10-fold cross-validation to assess the generalizability of the proposed methodology. Several other measures were calculated to assess the predictive performance. For multiclass classification, we calculated overall accuracy and precision. For binary classes, we calculated accuracy, sensitivity, specificity, and Matthews correlation coefficient (MCC) using eqs 3−6, respectively.

$$\text{Accuracy} = \frac{(\text{TP} + \text{TN})}{(\text{TP} + \text{FP} + \text{FN} + \text{TN})} \quad (3)$$

$$\text{Sensitivity} = \frac{(\text{TP})}{(\text{TP} + \text{FN})} \quad (4)$$

$$\text{Specificity} = \frac{(\text{TN})}{(\text{TN} + \text{FP})} \quad (5)$$

DOI: 10.1021/acs.iecr.8b06064
Ind. Eng. Chem. Res. 2019, 58, 11498−11505

MCC was calculated to evaluate the quality of binary classification and can vary from 0 to 1. An MCC value closer to 1 represents a better classifier (See eq 6).

$$\mathrm{MCC} = \frac{(\mathrm{TP} \times \mathrm{TN} - \mathrm{FP} \times \mathrm{FN})}{\sqrt{(\mathrm{TP} + \mathrm{FP}) \times (\mathrm{TP} + \mathrm{FN}) \times (\mathrm{TN} + \mathrm{FP}) \times (\mathrm{TN} + \mathrm{FN})}} \quad (6)$$

where considering one class as positives and the other as negatives, TP refers to true positives, TN refers to true negatives, FP refers to false positives, and FN refers to false negatives.

3.3. Binary versus Multiclass Classification. We have made a comparison between a total of 6 subject classes, viz., AD, HC, MCI, late MCI, PD, and SWEDD. On considering the three types of brain tissue, a total of 45 binary classes were formed (see Table 2). Similarly, three multiclass classifier models were also built. For binary comparison between subject classes, on considering the highest accuracy achieved using either of the brain tissue, our method achieved an average classification accuracy greater than 97% with MCC of 0.92. For 12/15 subject class comparisons, classification accuracy of over 99% was achieved. For multiclass classification, we found gray matter tissue to be the most suitable, achieving an overall accuracy greater than 87% with a precision of 83% (see Table 2).

4. DISCUSSION

In the past, mainly two types of approaches have been explored, viz., (i) whole brain analysis and (ii) analysis on automated or manually selected regions of interest (ROIs).

Automated or manual selection of ROIs is mostly dependent on the type of disease under consideration based on insights from the disease pathology. Since understanding the pathology of these diseases and their related biomarkers is still an active area of research, even though the selection of ROIs reduces the data dimensionality, the designed model for disease diagnosis is inherently biased. Chen et al. divided the brain into 116 ROIs and, using the pairwise ROIs Pearson product moment correlation coefficients, obtained classification accuracy of 87 and 95% for distinguishing AD vs MCI and MCI vs HC, respectively.[15] Cui et al. used a combination approach where fractional anisotropy and large deformation diffeomorphic metric mapping to extract subcortical volumetric features that were fed to a support vector machine that was able to distinguish amnestic MCI and HC patients with an accuracy of 90%.[16] Duchesne et al. obtained features only from the medial temporal lobe while distinguishing equal numbers of AD and HC subjects with an accuracy of 92%.[17] Similarly, Gerardin et al. obtained only features from the hippocampi using spherical harmonics coefficients and upon using the support vector machine obtained classification accuracies of 94 and 83% to distinguish AD vs HC and MCI vs HC, respectively (see Table 3).[18]

However, whole brain analysis is an unbiased approach that takes into account all the brain regions. The dimensionality of data and computational complexity becomes an issue. To mitigate this, feature selection criteria are used to reduce data dimensionality based on statistical inferences from the data.

Many machine-learning approaches such as Gaussian mixture model,[19] linear discriminant analysis,[20] Pearson correlation,[21] principal component analysis,[4] and self-organizing maps[5] have been employed for feature extraction. In this study, we have performed a whole-brain analysis using principal component analysis and used a reformulated version of Fisher discriminant ratio for multiclass classification using LSSVM.

Another impending issue is that most of the studies have been aimed at (1) differential diagnosis of NDs by comparing binary sets of subject classes and (2) understanding either AD or PD and their related counterparts. Recently, Zhu et al. made use of linear discriminant analysis and locality preserving projection for multiclass classification in AD diagnosis and achieved an accuracy of 68.31 ± 1.23 using MRI.[20] Similarly, Liu et al. reported classification accuracy of only 64.07 ± 4.76% for the multiclass diagnosis of AD using multimodal imaging.[22] Koikkalainen et al. used control subjects and subjects from four common types of dementia: (1) Alzheimer's disease, (2) frontotemporal dementia, (3) vascular dementia, and (4) dementia with Lewy bodies. They performed multiclass classification analysis using Disease State Index (DSI)[23] and achieved a classification accuracy of 51.6%.[24] More recently, Tong et al. using random under sampling boosting (RUSBoost) achieved multiclass classification accuracy of 75.2% using imaging and nonimaging features derived from Alzheimer's disease, frontotemporal lobe degeneration, dementia with Lewy bodies and vascular dementia, and patients with subjective memory complaints.[25] Tolonen et. al used a similar cohort of subjects and developed a tool called PredictND for multiclass neurodegenerative disease diagnosis using the similar patient cohort. Using random under sampling boosting algorithm they achieved multiclass classification accuracy of 82.3%.[26] Table 3 compares the results obtained using our study with that of the existing methods.

Through this work, we have tried to address several pertinent issues. First, MRIs are routinely performed to estimate the cognitive impairment. They are noninvasive, widely available, and inexpensive as compared to its counterparts such as PET, DTI, and others. Using MRIs, we have demonstrated the ability to assist in differential diagnosis with high precision and accuracy. This makes it an ideal choice to be adopted in a clinical setting. Second, most of the studies have been conducted using in-house patients. Since data sets for these studies are rarely made available in the public domain, it difficult to reproduce their results. To overcome this limitation, data sets from two public repositories, viz., the Alzheimer's Disease Neuroimaging Initiative and the Parkinson Progression Marker Initiative, have been used in this study. Information about the subjects' IDs and other related details have been provided in the Supporting Information. Third, we have performed differential diagnosis for two of the most prevalent disease classes, AD and PD, from their similar counterparts, MCI and SWEDDs. To the best of our knowledge, ours is the first study investigating machine-learning-based diagnosis for the two most common NDs, AD and PD, at once. Fourth, we purposely included images from multicenter, multivendor and those with variable field strengths. With this, we aimed to assess the generalizability of the proposed methodology and evaluate the potential of the developed algorithm as clinical decision support for routine diagnosis. Last, most of the studies have been focused on comparing only two subject classes at once, i.e., in terms of binary classes. This is useful to highlight differences between the classes under consideration. However, the real challenge is to be able to predict a subject class by treating it as a multiclass problem with humanlike diagnostic capabilities. Only a handful of studies have recently addressed this issue. Upon using our methodology, we have obtained accuracy of 87.89 ± 03.98% with a precision of

DOI: 10.1021/acs.iecr.8b06064
Ind. Eng. Chem. Res. 2019, 58, 11498−11505

82.54 ± 08.85%. This is the highest reported accuracy for multiclass classification of NDs.

5. CONCLUSION

In summary, MRIs, routinely performed for assessment of cognitive impairment of subjects could be processed using this method to obtain probable subject classification. The results obtained using the proposed methodology along with doctor consultation promises a new paradigm in medical technology for ND diagnosis (see Figure 3). The ease of applicability, adaptability to images from multiple scanners, and the high performance of the proposed methodology on the largest cohort of patients reported in the literature establishes the it as an ideal candidate for its transferability into a first-line neuroimaging diagnostic tool for NDs in a clinical setting.

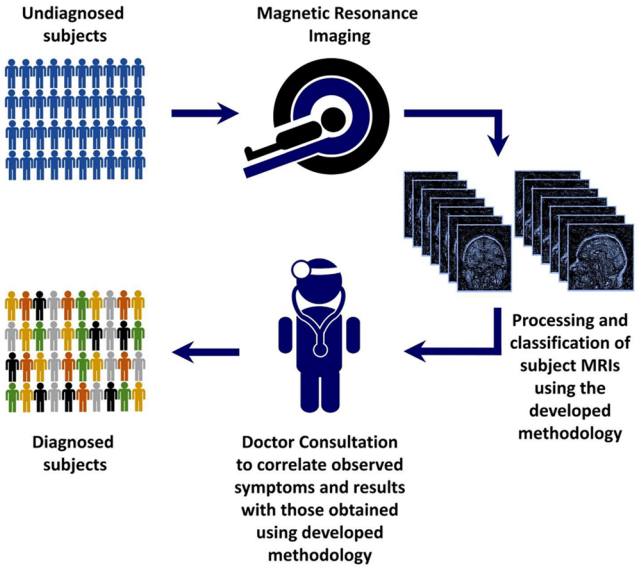

Figure 3. First-line neuroimaging diagnostic tool for a clinical setting.

■ ASSOCIATED CONTENT

Supporting Information

The Supporting Information is available free of charge on the ACS Publications website at DOI: 10.1021/acs.iecr.8b06064.

Table summarizing the accuracy rates obtained for binary comparison between subjects for each type of brain tissue (PDF)

Details regarding the patient used in this study (XLSX)

■ AUTHOR INFORMATION

Corresponding Author

*E-mail: laksh@nus.edu.sg. Phone: +65-98156213.

ORCID

Lakshminarayanan Samavedham: 0000-0003-4323-6315

Notes

†A preliminary version of this work was presented at 11th International Federation of Automatic Control−Symposium on Dynamics and Control of Process Systems, including Bio systems, June 6−8, 2016. Norwegian University of Science and Technology, Trondheim, Norway.[28]

The authors declare no competing financial interest.

■ ACKNOWLEDGMENTS

G.S. would like to acknowledge the support of the National University of Singapore by providing Research Scholarship towards the fulfillment of his Doctor of Philosophy degree. Data collection and sharing for this study was funded by the Alzheimer's Disease Neuroimaging Initiative and the Parkinson's Progression Markers Initiative primarily supported by the National Institute on Aging, the National Institute of Biomedical Imaging & Bioengineering and by the Michael J. Fox Foundation for Parkinson's Research, respectively. These investigators only provided the data, and they did not contribute toward its analysis or writing of this manuscript.

■ ABBREVIATIONS

AD = Alzheimer's disease
HC = Healthy control
LMCI = Late mild cognitive impairment
MCC = Matthews correlation coefficient
MCI = Mild cognitive impairment
ND = Neurodegenerative diseases
PD = Parkinson's disease
ROI = Region of interest
SWEDD = Scans without evidence of dopaminergic deficit

■ REFERENCES

(1) Prince, M.; Wimo, A.; Guerchet, M.; Gemma-Claire, A.; Wu, Y.-T.; Prina, M. World Alzheimer Report 2015: The Global Impact of Dementia - An Analysis of Prevalence, Incidence, Cost and Trends. *Alzheimer's Dis. Int.*, **2015**, *84*. DOI: 10.1111/j.0963-7214.2004.00293.x.

(2) Mueller, S. G.; Schuff, N.; Weiner, M. W. Evaluation of Treatment Effects in Alzheimer's and Other Neurodegenerative Diseases by MRI and MRS. *NMR Biomed.* **2006**, *19* (6), 655−668.

(3) Seppi, K.; Poewe, W. Brain Magnetic Resonance Imaging Techniques in the Diagnosis of Parkinsonian Syndromes. *Neuroimaging Clin. N. Am.* **2010**, *20* (1), 29−55.

(4) Salvatore, C.; Cerasa, A.; Castiglioni, I.; Gallivanone, F.; Augimeri, A.; Lopez, M.; Arabia, G.; Morelli, M.; Gilardi, M. C.; Quattrone, A. Machine Learning on Brain MRI Data for Differential Diagnosis of Parkinson's Disease and Progressive Supranuclear Palsy. *J. Neurosci. Methods* **2014**, *222*, 230−237.

(5) Singh, G.; Samavedham, L. Unsupervised Learning Based Feature Extraction for Differential Diagnosis of Neurodegenerative Diseases: A Case Study on Early-Stage Diagnosis of Parkinson Disease. *J. Neurosci. Methods* **2015**, *256*, 30−40.

(6) Shi, B.; Wang, Z.; Liu, J. Distance-Informed Metric Learning for Alzheimer's Disease Staging. *36th Annu. Int. Conf. IEEE Eng. Med. Biol. Soc.* **2014**, 934−937.

(7) Vemuri, P.; Gunter, J. L.; Senjem, M. L.; Whitwell, J. L.; Kantarci, K.; Knopman, D. S.; Boeve, B. F.; Petersen, R. C.; Jack, C. R. Alzheimer's Disease Diagnosis in Individual Subjects Using Structural MR Images: Validation Studies. *NeuroImage* **2008**, *39* (3), 1186−1197.

(8) Focke, N. K.; Helms, G.; Pantel, P. M.; Scheewe, S.; Knauth, M.; Bachmann, C. G.; Ebentheuer, J.; Dechent, P.; Paulus, W.; Trenkwalder, C. Differentiation of Typical and Atypical Parkinson Syndromes by Quantitative MR Imaging. *Am. J. Neuroradiol.* **2011**, *32* (11), 2087−2092.

(9) Pennington, B. F.; Filipek, P. A.; Lefly, D.; Chhabildas, N.; Kennedy, D. N.; Simon, J. H.; Filley, C. M.; Galaburda, A.; DeFries, J. C. A Twin MRI Study of Size Variations in the Human Brain. *J. Cogn. Neurosci.* **2000**, *12* (1), 223−232.

(10) Mazziotta, J. C.; Toga, A. W.; Evans, A.; Fox, P.; Lancaster, J. A Probabilistic Atlas of the Human Brain: Theory and Rationale for Its Development. *NeuroImage* **1995**, *2* (2), 89−101.

(11) Ashburner, J.; Friston, K. J. Voxel-Based Morphometry - The Methods. *NeuroImage* **2000**, *11* (6I), 805−821.

(12) Penny, W.; Friston, K.; Ashburner, J.; Kiebel, S.; Nichols, T.. *Statistical Parametric Mapping: The Analysis of Funtional Brain Images*; Elsevier/Academic Press, 2007.
(13) Chu, C.; Hsu, A. L.; Chou, K. H.; Bandettini, P.; Lin, C. Does Feature Selection Improve Classification Accuracy? Impact of Sample Size and Feature Selection on Classification Using Anatomical Magnetic Resonance Images. *NeuroImage* **2012**, *60* (1), 59−70.
(14) Suykens, J. A. K.; Vandewalle, J. Least Squares Support Vector Machine Classifiers. *Neural Process. Lett.* **1999**, *9* (3), 293−300.
(15) Chen, G.; Ward, B. D.; Xie, C.; Li, W.; Wu, Z.; Jones, J. L.; Franczak, M.; Antuono, P.; Li, S. J. Classification of Alzheimer Disease, Mild Cognitive Impairment, and Normal Cognitive Status with Large-Scale Network Analysis Based on Resting-State Functional MR Imaging. *Radiology* **2011**, *259* (1), 213−221.
(16) Cui, Y.; Wen, W.; Lipnicki, D. M.; Beg, M. F.; Jin, J. S.; Luo, S.; Zhu, W.; Kochan, N. A.; Reppermund, S.; Zhuang, L.; et al. Automated Detection of Amnestic Mild Cognitive Impairment in Community-Dwelling Elderly Adults: A Combined Spatial Atrophy and White Matter Alteration Approach. *NeuroImage* **2012**, *59* (2), 1209−1217.
(17) Duchesne, S.; Caroli, A.; Geroldi, C.; Barillot, C.; Frisoni, G. B.; Collins, D. L. MRI-Based Automated Computer Classification of Probable AD versus Normal Controls. *IEEE Trans. Med. Imaging* **2008**, *27* (4), 509−520.
(18) Gerardin, E.; Chételat, G.; Chupin, M.; Cuingnet, R.; Desgranges, B.; Kim, H. S.; Niethammer, M.; Dubois, B.; Lehéricy, S.; Garnero, L.; et al. Multidimensional Classification of Hippocampal Shape Features Discriminates Alzheimer's Disease and Mild Cognitive Impairment from Normal Aging. *NeuroImage* **2009**, *47* (4), 1476−1486.
(19) Salas-Gonzalez, D.; Górriz, J. M.; Ramírez, J.; Illán, I. A.; López, M.; Segovia, F.; Chaves, R.; Padilla, P.; Puntonet, C. G. Feature Selection Using Factor Analysis for Alzheimer's Diagnosis Using F 18 -FDG PET Images. *Med. Phys.* **2010**, *37* (11), 6084−6095.
(20) Zhu, X.; Suk, H. Il; Lee, S. W.; Shen, D. Subspace Regularized Sparse Multitask Learning for Multiclass Neurodegenerative Disease Identification. *IEEE Trans. Biomed. Eng.* **2016**, *63* (3), 607−618.
(21) Graña, M.; Termenon, M.; Savio, A.; Gonzalez-Pinto, A.; Echeveste, J.; Pérez, J. M.; Besga, A. Computer Aided Diagnosis System for Alzheimer Disease Using Brain Diffusion Tensor Imaging Features Selected by Pearson's Correlation. *Neurosci. Lett.* **2011**, *502* (3), 225−229.
(22) Liu, S.; Liu, S.; Cai, W.; Che, H.; Pujol, S.; Kikinis, R.; Feng, D.; Fulham, M. J.; Adni. Multimodal Neuroimaging Feature Learning for Multiclass Diagnosis of Alzheimer's Disease. *IEEE Trans. Biomed. Eng.* **2015**, *62* (4), 1132−1140.
(23) Mattila, J.; Koikkalainen, J.; Virkki, A.; Van Gils, M.; Lötjönen, J. Design and Application of a Generic Clinical Decision Support System for Multiscale Data. *IEEE Trans. Biomed. Eng.* **2012**, *59*, 234.
(24) Koikkalainen, J.; Rhodius-Meester, H.; Tolonen, A.; Barkhof, F.; Tijms, B.; Lemstra, A. W.; Tong, T.; Guerrero, R.; Schuh, A.; Ledig, C. Differential Diagnosis of Neurodegenerative Diseases Using Structural MRI Data. *Neuro Image Clin.* **2016**, *11*, 435.
(25) Tong, T.; Ledig, C.; Guerrero, R.; Schuh, A.; Koikkalainen, J.; Tolonen, A.; Rhodius, H.; Barkhof, F.; Tijms, B.; Lemstra, A. W. Five-Class Differential Diagnostics of Neurodegenerative Diseases Using Random Undersampling Boosting. *Neuro Image Clin.* **2017**, *15*, 613.
(26) Tolonen, A.; Rhodius-Meester, H. F. M.; Bruun, M.; Koikkalainen, J.; Barkhof, F.; Lemstra, A. W.; Koene, T.; Scheltens, P.; Teunissen, C. E.; Tong, T. Data-Driven Differential Diagnosis of Dementia Using Multiclass Disease State Index Classifier. *Front. Aging Neurosci.* **2018**, *10*, 111 DOI: 10.3389/fnagi.2018.00111.
(27) Plant, C.; Teipel, S. J.; Oswald, A.; Böhm, C.; Meindl, T.; Mourao-Miranda, J.; Bokde, A. W.; Hampel, H.; Ewers, M. Automated Detection of Brain Atrophy Patterns Based on MRI for the Prediction of Alzheimer's Disease. *NeuroImage* **2010**, *50* (1), 162−174.
(28) Singh, G.; Vadera, M.; Samavedham, L.; Lim, E. C. H. Machine Learning-Based Framework for Multi-Class Diagnosis of Neuro-degenerative Diseases: A Study on Parkinson's Disease. *IFAC-Papers Online* **2016**, *49*, 990.

DOI: 10.1021/acs.iecr.8b06064
Ind. Eng. Chem. Res. 2019, 58, 11498−11505